Neuron
Article

# GABA Neurons of the VTA Drive Conditioned Place Aversion

Kelly R. Tan,[1] Cédric Yvon,[1,6] Marc Turiault,[1,6] Julie J. Mirzabekov,[2] Jana Doehner,[3] Gwenaël Labouèbe,[1] Karl Deisseroth,[2] Kay M. Tye,[2,4] and Christian Lüscher[1,5,*]
[1]Department of Basic Neurosciences, University of Geneva, 1211 Geneva, Switzerland
[2]Department of Bioengineering, Stanford University, Stanford, CA 94305, USA
[3]Institute of Pharmacology and Toxicology, University of Zurich, 8057 Zurich, Switzerland
[4]Picower Institute of Learning and Memory, Brain and Cognitive Sciences, Massachusetts Institute of Technology, Cambridge, MA 02139, USA
[5]Clinic of Neurology, University Hospital of Geneva, 1211 Geneva, Switzerland
[6]These authors contributed equally to this work
*Correspondence: christian.luscher@unige.ch
DOI 10.1016/j.neuron.2012.02.015

## SUMMARY

**Salient but aversive stimuli inhibit the majority of dopamine (DA) neurons in the ventral tegmental area (VTA) and cause conditioned place aversion (CPA). The cellular mechanism underlying DA neuron inhibition has not been investigated and the causal link to behavior remains elusive. Here, we show that GABA neurons of the VTA inhibit DA neurons through neurotransmission at $GABA_A$ receptors. We also observe that GABA neurons increase their firing in response to a footshock and provide evidence that driving GABA neurons with optogenetic effectors is sufficient to affect behavior. Taken together, our data demonstrate that synaptic inhibition of DA neurons drives place aversion.**

## INTRODUCTION

The mesocorticolimbic dopamine system originates in the VTA and drives reward-related behavior (Fields et al., 2007; Sun, 2011). The VTA is a heterogeneous nucleus containing DA neurons (~65%), GABA neurons (~30%) (Dobi et al., 2010), and glutamatergic neurons (~5%) (Yamaguchi et al., 2007). DA is thought to represent a teaching signal and has also been implicated in the induction of addictive behaviors (Lüscher and Malenka, 2011).

In fact, many VTA DA neurons are activated by reward or a cue-predicting the reward. In both cases, DA neuron firing increases only if the salient stimulus occurs without anticipation (Schultz et al., 1997). In contrast, DA neurons are inhibited by reward omission. Based on these observations, now confirmed across several species ranging from humans (D'Ardenne et al., 2008) to rats (Flagel et al., 2011), it is generally accepted that DA neuron firing codes for the prediction error of reward.

However, several studies reported that salient but aversive stimuli can enhance DA neuron activity (reviewed in Salamone, 1994, and Pezze and Feldon, 2004), that DA receptor antagonist can blunt behavioral impact (Acquas et al., 1989), and that genetic manipulations of DA signaling interfere with acquisition and expression of aversive conditioning (Fadok et al., 2009, 2010). These studies have challenged the exclusive role of the mesolimbic DA system in reward processing. Additional evidence shows that the firing of some DA neurons, which are typically located in the caudal VTA, increased briefly in response to a footshock (Brischoux et al., 2009). Moreover, VTA DA neurons can also be activated by conditioned aversive stimuli (Guarraci et al., 1999), restraint stress (Anstrom and Woodward, 2005), or social defeat stress (Anstrom et al., 2009). Clearly, VTA DA neurons are by no means a homogenous population, but subserve contrasting function in motivational control through connections with distinct circuits. As stated in a recent review, "some DA neurons encode motivational value, supporting brain networks for seeking, evaluation, and value learning. Others encode motivational salience, supporting brain networks for orienting, cognition, and general motivation" (Bromberg-Martin et al., 2010a).

The control of DA neuron activity and the ensuing changes in DA levels in the target regions of the VTA are therefore important for the control of behavior. How DA levels can increase has been studied extensively. For example, addictive drugs raise DA through distinct cellular mechanisms (Lüscher and Ungless, 2006), one of which involves the disinhibition of DA neurons via an inhibition of local VTA GABA neurons (Cruz et al., 2004; Labouèbe et al., 2007; Tan et al., 2010). It may therefore be the case that aversive stimuli activate VTA GABA neurons to transiently suppress DA neuron activity, which determines the behavioral response.

It has been shown that salient but aversive stimuli can in fact strongly inhibit DA neurons in the VTA (Ungless et al., 2004; Hong et al., 2011). Recent investigations into the origins of this response have identified two nuclei in rats and monkeys, the lateral habenula and the rostromedial tegmental nucleus (RMTg), which may play a role in DA neuron responses to aversive stimuli (Hong et al., 2011; Jhou et al., 2009a). This mirrors the established role of the VTA in reward processing (Fields et al., 2007; Schultz, 2010). However, due to the technical difficulties, it has until now been impossible to dissect the role of

VTA GABA neurons in the control of DA neurons during aversive events. Here, we take advantage of in vivo electrophysiology and cell-type-specific expression of optogenetic effectors to probe the role of VTA GABA neurons in mediating DA neuron inhibition. We further investigate the role of VTA GABA neurons in an electric footshock-induced inhibition of DA neurons and test whether activation of VTA GABA neurons is sufficient to elicit avoidance behavior.

## RESULTS

### Optogenetic Activation of VTA GABA Neurons Inhibits DA Neurons

We expressed the optogenetic effector channelrhodopsin-2 (ChR2) selectively in GABA neurons of the VTA by injecting an adeno-associated virus (serotype 5) containing a double-floxed inverted open reading frame encoding a fusion of ChR2 and enhanced yellow fluorescent protein (ChR2-eYFP) into the VTA of transgenic mice expressing cre recombinase in GAD65-positive neurons (Kätzel et al., 2011). Functional ChR2-eYFP is transcribed only in neurons containing Cre, thus restricting expression to GABA neurons of the VTA. To validate this approach, we performed immunohistochemistry on VTA slice from infected GADcre$^{+}$ mice and observed that ChR2-eYFP was selectively expressed in GABA neurons. This conclusion is based on the eYFP colocalization with the $\alpha$1 subunit isoform of the $GABA_A$ receptor (Tan et al., 2010) and mutual exclusion of tyrosine hydroxylase (TH) staining (Figure 1A). The quantification revealed that 92% of the GABA neurons expressed the ChR2-eYFP, while this was the case only in 3% of the DA neurons (inset, Figure 1A). The expression of the ChR2-eYFP was restricted to the VTA (Figure 1B). In vitro patch-clamp recordings also confirmed a selective expression of ChR2-eYFP in GABA cells and a synaptic connection of the latter with DA neurons as inhibitory light evoked current recorded from DA cells were abolished with picrotoxin (see Figure S1 available online; van Zessen et al., 2012, this issue of *Neuron*). Two weeks after the infection, anesthetized mice were canulated (Figures 1B and 1C) and GABA neuron firing controlled with blue-light (Figures 1D–1H). Intermitted blue-light stimulation (20 Hz, 5 pulses, data not shown) or continuous illumination for one second reliably excited GABA neurons as monitored by extracellular single unit recordings in vivo (+560% ± 174%; Figures 1D, 1F, and 1G). As a consequence DA neurons were strongly inhibited (−88% ± 5%; Figures 1E, 1F, and 1H). In absolute values at baseline the firing frequency was 2.08 ± 2.45 Hz on average, while during stimulation 11.85 ± 10.06 Hz was measured (n = 10, data not shown). Taken together, selective activation of VTA GABA neurons leads to the inhibition of DA neurons similar to the inhibition observed by an electric footshock.

### Effect of a Footshock on VTA Cells

Since VTA GABA neurons inhibit strongly the activity of DA neurons, we hypothesized that the footshock-induced inhibition of DA neurons is caused by the excitation of VTA GABA neurons. We then performed recordings in vivo from VTA neurons of wild-type (WT) anaesthetized mice. One brief electric footshock (0.1 ms, 1–5 mA) sufficient to cause aversion in freely moving animals (Valenti et al., 2011; Rosenkranz et al., 2006) induced opposite responses on the spontaneous firing of putative DA neurons and putative GABA neurons of the VTA, which were identified by the criteria detailed below. Whereas putative DA neurons were inhibited, putative GABA neurons were excited (Figures 2A, 2B, and 2D). We also recorded occasional DA neurons that were excited by the footshock (Figures 2C and 2D). These cells were typically located in the medial, ventral, and caudal portion of the VTA (Brischoux et al., 2009). Here, we focused our study on the cells that were inhibited by a footshock. The average response duration of the putative GABA neurons was longer than in the putative DA neurons (485 ± 345 ms versus 194 ± 131 ms, respectively; Figures 2E and 2F) while the average response latency was also significantly delayed in putative DA neurons compared to putative GABA neurons (38 ± 38 ms versus 18 ± 17 ms; Figures 2E and 2F). Interestingly, the activation of the putative GABA neurons occurred in several waves, which were mirrored by an inhibition of putative DA neurons that was initially complete and then gradually recovered. Such oscillation may originate in excitatory input onto GABA neurons, or their connectivity via gap junctions (Lassen et al., 2007) and may be part of multiplexed timing mechanisms recently reported in the mesolimbic DA system that supports processing of information (Fujisawa and Buzsáki, 2011). Recurring activity was first observed during a trough of the GABA activity until reaching baseline within one second (Figure 2F). Taken together, these data suggest that putative GABA neurons of the VTA mediate the inhibition of putative DA neurons, when activated by aversive stimuli.

The identification of VTA neurons was based on their established pharmacological signature and electrophysiological properties (Figure S2). A neuron was categorized as putative DA when it was disinhibited by morphine and inhibited by apomorphine (Beckstead et al., 2004; Figures S2A and S2C). Conversely, putative GABA neurons were inhibited by morphine (Johnson and North, 1992, Figures S2B and S2C).

In addition, putative DA neurons exhibited (1) a slow firing rate below 10 Hz with occasional slow bursting activity (Figure S2D; Grace and Bunney, 1983), (2) an action potential width to the trough larger than 1.1 ms (Ungless et al., 2004) and a regular firing rate (Figure S2E), (3) a total duration of the action potential longer than 2.0 ms (Luo et al., 2008; Figure S2E). The putative DA and GABA neurons recorded in this study were located throughout the VTA. However, some of the putative GABA neurons were located in more dorsal parts of the VTA (Figure S2F).

### $GABA_A$ Receptor Mediates the Footshock-Driven Inhibition of DA Neurons

We next aimed at identifying the neurochemical basis of the footshock-driven inhibition of DA neurons. Several effector systems can efficiently hyperpolarize DA neurons to inhibit firing, including G protein inwardly rectifying potassium (GIRK) channels active in response to D2 autoreceptor or $GABA_B$ heteroreceptor activation as well as $GABA_A$ receptors. In mice lacking the GIRK subunits expressed in DA neurons (Cruz et al., 2004), putative DA neurons were still inhibited by a footshock (latency: WT 30 ± 32 ms versus GIRK2/3 KO 46 ± 41 ms;

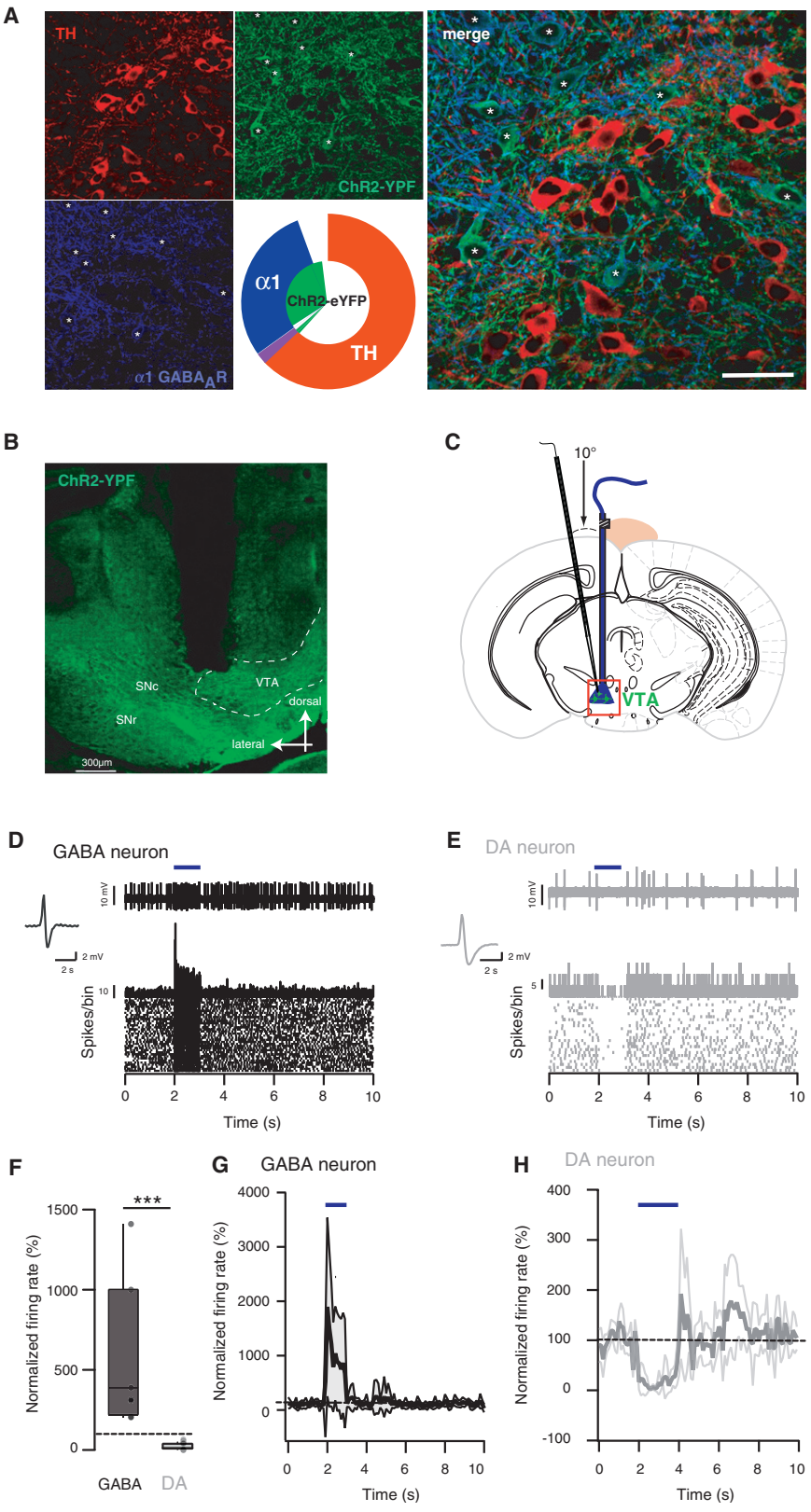


**Figure 1. Excitation of GABA Neurons In Vivo Inhibits DA Neurons of the VTA**

(A) Immunohistochemical staining for tyrosine hydroxylase (TH, red) and α1 subunit isoform of the $GABA_A$ receptor (blue, soma highlighted with stars) in VTA slices of $GADcre^+$ mice infected with AAV5-flox-ChR2-YFP (green) in the VTA. Concentric pie charts represent the fraction of ChR2-YFP-positive cells (inner segment) and quantification of the two cell types (outer segment, n = 4 mice). Overlap between inner and outer segments represents colocalization (violet color represents colocalization of TH and GAD).

(B) Coronal slice of a VTA expressing ChR2-eYFP in GABA cells showing the restriction of the expression of ChR2-eYFP to the VTA and the path of the guide cannula down to the VTA. Substantia nigra compacta and reticulata (SNc/SNr).

(C) Schematic showing the positioning of the in vivo recording pipette relative to the optic fiber. A guide cannula was stereotaxically implanted in vivo above a VTA expressing ChR2-eYFP in GABA cells. The recording pipette was then lowered down to the VTA with a 10°C angle to avoid contact with the guide cannula. The red box locates the image shown in (B).

(D) Single-unit recording, PSTH and raster plot of a ChR2-eYFP-expressing GABA neuron excited by a blue light stimulation for 1 s.

(E) Same as in (D) for non ChR2-eYFP-expressing DA neuron inhibited by a 1 s blue light stimulation.

(F) Boxplot representation showing the relative effect of 1 and 2 s blue light stimulation on GABA and DA neurons, respectively ***$p \leq 0.001$ n = 8–12.

(G) Normalized firing rate of GABA neurons that were excited during the 1 s blue light stimulation. The black trace shows the average for 8 cells and the gray area correspond to the SD.

(H) Normalized firing rate of DA neurons that were inhibited during the 2 s blue light stimulation. The gray trace shows the average for 12 cells and the light gray area correspond to the SD.

See also Figure S1.

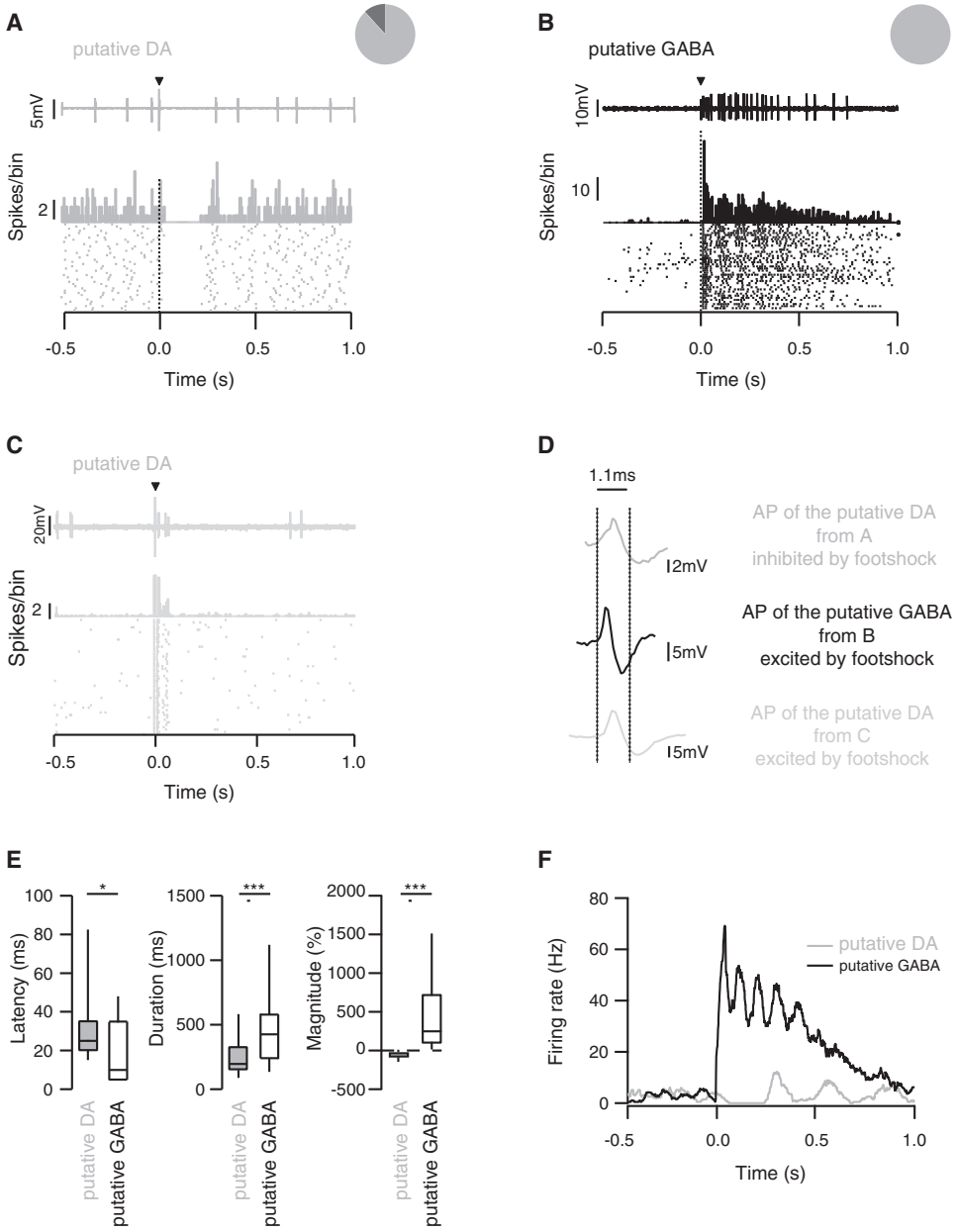


**Figure 2. Effect of Electrical Footshock on Spontaneous Activity of VTA Neurons**

(A) Single-unit recording, peristimulus histograms (PSTH), and raster plot of a typical putative DA neuron inhibited by a single electrical footshock. The inset shows that 90% of the recorded cells were inhibited whereas the other 10% did not respond.

(B) Same as in (A) for a putative GABA neuron, which is excited by the stimulus. The pie chart shows that the footshock stimulation induced an excitation of all GABA neurons.

(C) Same as in (A) and (B) for a putative DA neuron, which is excited by the stimulus. This putative DA cell population represents a minority of recorded putative DA cells.

(D) Average action potential waveform from the three representative cells in (A), (B), and (C). The vertical dotted lines represent the limit (1.1 ms) for which a cell is considered a DA or a GABA cell.

(E) Boxplot representation of latency $t_{(70)} = 2.3$ *$p < 0.01$, response duration $t_{(77)} = 3.52$ ***$p < 0.01$ and response magnitude $t_{(46)} = 5.98$ ***$p < 0.01$ for putative DA and GABA neurons, n = 21–56. Data are expressed as median (line), interquartile (box) 75$^{th}$ and 25$^{th}$ percentiles, and SD (error bars).

(F) Example of effects of a single electrical footshock on the firing rate of a putative GABA and a putative DA neuron.

See also Figure S2.

duration: WT 266 ± 159 ms versus GIRK2/3 KO 335 ± 192 ms; magnitude: WT −53% ± 35% versus GIRK2/3 KO −46% ± 19%; Figures 3A and 3B). It has been previously suggested that inhibition of DA neurons can be mediated by the activation of D2 autoreceptors after somatodendritic release of dopamine (Beckstead et al., 2004). To test this possibility, we monitored footshock responses before and after i.v. injection of the DA receptor antagonist haloperidol. Again, this manipulation had no effect on the footshock inhibition of DA neurons (latency: saline 36 ± 25 ms versus haloperidol 30 ± 18 ms; duration: saline 215 ± 105 ms versus haloperidol 201 ± 91 ms; magnitude: saline −55% ± 13% versus haloperidol −53% ± 16%; Figures 3C and 3D).

Finally, we investigated the contribution of $GABA_A$ receptors to the suppression of firing in putative DA cells (Figures 3E–3G and S3; van Zessen et al., 2012). We found that neurons recorded with bicuculline-filled electrodes had significantly higher firing rate (saline: 4.78 ± 2.26 Hz, n = 35; bicuculline: 6.17 ± 2.26 Hz, n = 35, p = 0.013) as well as a higher bursting activity (saline: 18.7% ± 21.6%; bicuculline: 39.0% ± 26.1%, p < 0.001, data not shown). These results confirm that the drug diffusion in the vicinity of the cell was efficiently blocking $GABA_A$ receptors. Whereas 88% of the cells (30 out of 34) were initially inhibited under control conditions (Figure S3A), this proportion decreased to 42% (14 out of 33) when bicuculline-loaded electrodes were used (Figure S3A and S3B, insets). The residual footshock-induced inhibition still observed in these 14 cells may be due to limited diffusion of bicuculline (Figure S3C). We therefore repeated the experiment with bicuculline applied via a guide cannula that was implanted above the VTA of anaesthetized mice (Figures 1C and 3E–3G). In these conditions, 90% of the recorded DA neurons no longer responded to the footshock (latency: saline 47 ± 33 ms versus bicuculline 1 ± 1 ms; duration: saline 285 ± 62 ms versus bicuculline 1 ± 1 ms; and magnitude: saline −100% ± 28% versus bicuculline −5% ± 5%, Figure 3G).

### Optogenetic Activation of VTA GABA Neurons Is Sufficient to Drive Conditioned Place Aversion

Given that a salient but aversive stimulus excites VTA GABA neurons that then inhibits DA neurons also causes aversion, we tested whether the exogenous excitation of VTA GABA neurons is sufficient to induce this behavior. To this end we looked for conditioned place aversion in ChR2-eYFP-VTA infected and cannulated GADcre$^+$ and GADcre$^-$ mice (Figures 4 and S4). The protocol lasted 4 days and mice always had free access to the whole apparatus (Figure S4A). During the conditioning sessions, a blue light laser was switched on whenever the mouse entered the conditioned chamber. Already during the first conditioning session, this manipulation caused a strong aversion of the chamber where the laser was active in GADcre$^+$ mice (pretest day GADcre$^+$ 50.4% ± 2.5% versus conditioning day 1 GADcre$^+$ 23.6% ± 5.6%; conditioning day 1 GADcre$^-$ 61.2% ± 5.8% versus conditioning day 1 GADcre$^+$ 23.6% ± 5.6%; Figure 4A). On the test day, in the absence of blue light stimulation, GADcre$^+$ mice developed an aversion for the light-paired chamber (pretest day GADcre$^+$ 6.9 ± 36.6 s versus test day GADcre$^+$ −385.8 ± 64.3 s; test day GADcre$^-$ −2.2 ± 52.9 s versus test day GADcre$^+$ −385.8 ± 64.3 s; Figures 4B and 4C).

Furthermore, during the conditioning sessions, mice were hesitant to enter the conditioned chamber and displayed a U-turn behavior never observed at the entry of the unconditioned chamber (U-turns count conditioned chamber GADcre$^+$ 3.7 ± 1.2 s versus unconditioned chamber GADcre$^+$ 0 ± 0; conditioned chamber GADcre$^+$ 3.7 ± 1.2 s versus conditioned chamber GADcre$^-$ 0.3 ± 0.2; Figure 4D). When they actually entered the conditioned chamber they moved significantly faster (test day GADcre$^+$ 0.08 ± 0.01 m/s versus GADcre$^-$ 0.05 ± 0.01 m/s; Figures 4E and S4B) to escape to the nonconditioned chamber where they showed a freezing behavior (test day GADcre$^+$ 170.5 ± 51.7 s versus GADcre$^-$ 34.5 ± 11.8 s; Figures 4F and S4C). To confirm that inhibition of VTA DA neurons is responsible for the development of the operant CPA, we repeated the experiment in THcre$^+$ mice where the VTA was infected with an AAV (serotype 5) expressing double-floxedzDIO-eNpHR3.0-eYFP. As a control group, THcre$^+$ mice were infected with an AAV5-DIO-eYFP. Immunohistochemistry showed a 96% colocalization of TH and eNpHR3.0-eYFP (Figure S4E) restricted to the VTA (Figure S4F). We then repeated the operant CPA protocol with the THcre/eNpHR3.0-eYFP mice. Venturing into the conditioned chamber triggered an amber laser, which led to an aversion of the light-paired chamber already during the conditioning sessions (pretest day THcre/eNpHR3.0-eYFP 49.6% ± 4.5% versus conditioning day 2 THcre/eNpHR3.0-eYFP 29.0% ± 4.2%; conditioning day 2 THcre/eYFP 46.3% ± 5.8% versus conditioning day 2 THcre/eNpHR3.0 29.0% ± 4.2%; Figure 4G). On the test day, with the amber laser no longer active, THcre/eNpHR3.0-eYFP mice retained an aversion for the light paired-chamber (pretest day THcre/eNpHR3.0-eYFP 2.6 ± 70.1 s versus test day THcre/eNpHR3.0-eYFP −276.4 ± 81.5 s; test day THcre/eYFP 36.3 ± 109.1 s versus test day THcre/eNpHR3.0-eYFP 276.4 ± 81.5 s; Figure 4H). Interestingly, the CPA score was almost identical to the one observed with GADcre$^+$/ChR2-eYFP mice. The control mice groups for both conditions were indifferent to all manipulations throughout the duration of the experiment (Figures 4 and S4). Importantly, the blue and amber light stimulations did not have an impact on the overall locomotor activity, as the total distance traveled was similar in all groups (Figures S4D and S4G).

## DISCUSSION

Here, we show that optogenetic activation of VTA GABA neurons inhibits DA neurons of the VTA. We then provide evidence that VTA GABA neurons also inhibit DA neurons in response to a brief footshock via $GABA_A$ transmission. Finally, we observe that activation of VTA GABA neuron or direct inhibition of DA neurons is sufficient to elicit a strong place aversion. These findings are in line with the companion paper in this issue of *Neuron* (van Zessen et al., 2012).

The inhibitory synaptic networks that control DA neuron's activity are increasingly well described. GABA neurons of the VTA receive inhibitory afferents from medium spiny neurons of the nucleus accumbens (Xia et al., 2011). If a footshock leads to a decrease in MSN activity, this could cause the disinhibition of VTA GABA neurons and eventually inhibition of DA neurons.

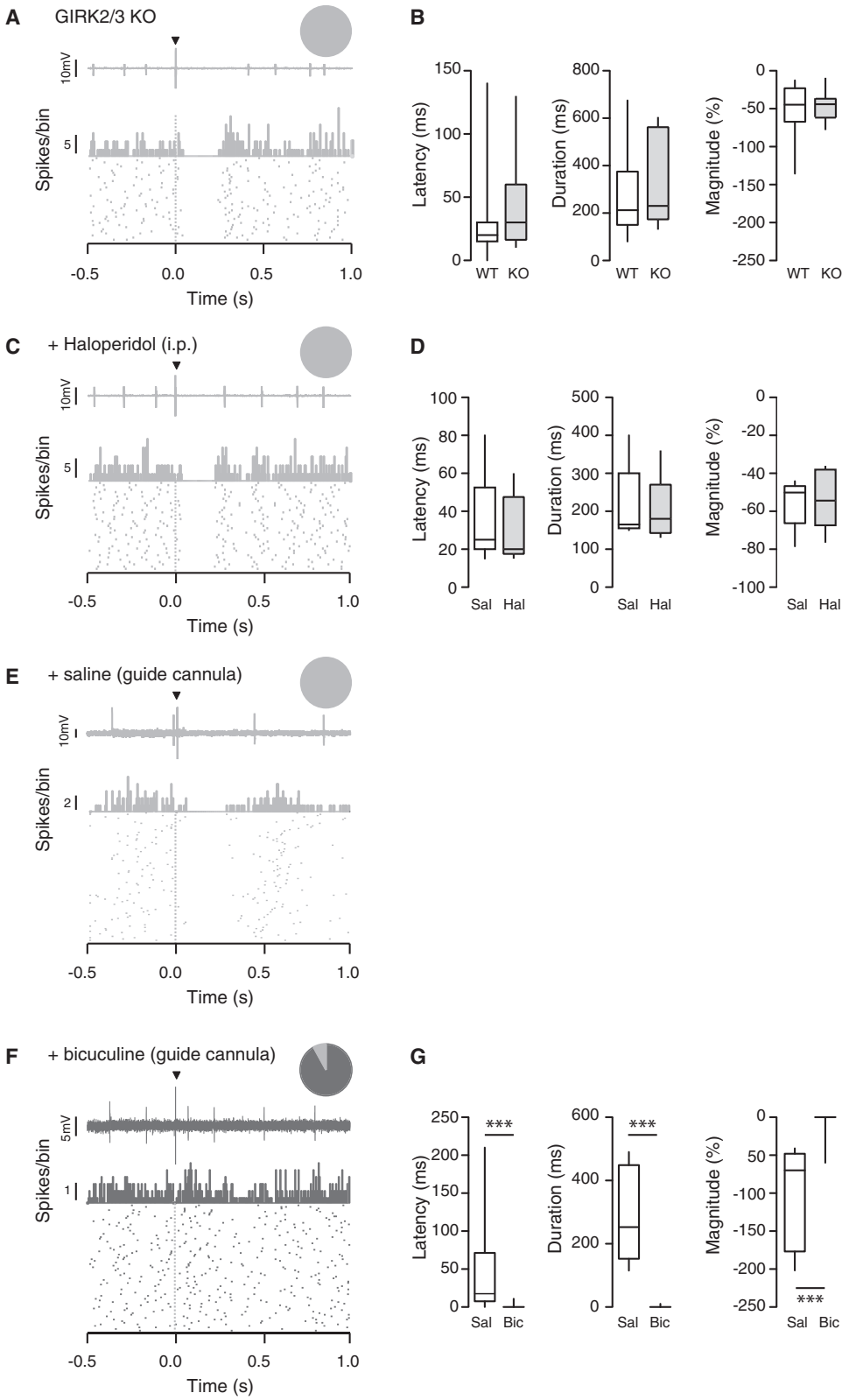
A
GIRK2/3 KO
10mV
Spikes/bin
5
-0.5
0.0
0.5
1.0
Time (s)
B
Latency (ms)
Duration (ms)
Magnitude (%)
WT
KO
C
+ Haloperidol (i.p.)
D
Sal
Hal
E
+ saline (guide cannula)
2
F
+ bicuculine (guide cannula)
5mV
1
G
***
Bic

This however seems unlikely as a tail pinch causes, on the contrary, an excitation of striatal units and would have an effect with a longer latency (Williams and Millar, 1990). Alternatively, an increased excitatory drive may be responsible for the enhanced GABA neuron activity. In rats, the lateral habenula sends excitatory inputs onto GABA neurons clustered in the tail of the VTA termed RMTg nucleus (Ji and Shepard, 2007). These neurons have been demonstrated to impinge on VTA-DA neurons (Jhou et al., 2009b; Kaufling et al., 2009). Functionally, when the RMTg is surgically lesioned, the response to aversive stimuli is attenuated, which suggests a convergence of aversive inputs onto the RMTg (Jhou et al., 2009a). The GABA neurons recorded and stimulated in the present study are located throughout the VTA, albeit with a somewhat higher density toward dorsal and caudal parts of the VTA. Whether these GABA neurons in the mouse represent ''ectopic'' RMTg neurons or actual VTA interneurons remains a semantic question. More importantly, the upstream structures that drive their activity will have to be identified. It will be interesting to explore whether all VTA GABA neurons receive direct excitatory inputs from the lateral habenula, as has been demonstrated for the RMTg neurons in rats (Hong et al., 2011; Balcita-Pedicino et al., 2011).

Our data indicate that the footshock-induced DA neuron inhibition primarily relies on $GABA_A$ receptor transmission (van Zessen et al., 2012). Neither $GABA_B$ receptors nor D2 receptors, both present on DA neurons and reported to mediate a slow IPSC (Cruz et al., 2004; Beckstead et al., 2004), seem to play an important role.

Anatomical studies have also identified a small number of VTA GABA neurons that project to the nucleus accumbens. Our optogenetic manipulation most likely also activated these neurons. However, given their small number (Xia et al., 2011), it is unlikely that they would significantly contribute to the behavioral effects. It is also possible that their contribution may be masked when most DA neurons are inhibited, as in the experiments presented here. In fact, the observation of the behavioral effect was very similar in magnitude as well as the timing with which the aversion was induced; suggesting that the two manipulations have a very similar effect on the circuit that mediates this behavior. While there is heterogeneity among DA neurons, inhibiting the majority either directly or indirectly causes strong aversion.

Taken together, VTA GABA neurons, when activated optogenetically, may mimic the contextual aversion typically observed with a footshock. A brief electric shock to the paw is indeed a strongly aversive stimulus for a mouse that initially causes a flight behavior, followed by place aversion and freezing, particularly when the setting precludes an escape (Lázaro-Muñoz et al., 2010). The freezing behavior observed in the unconditioned chamber may reflect a state of generalized anxiety. Interestingly a similar observation was made when mice with decreased DA neuron excitability were exposed to repetitive footshocks (Zweifel et al., 2011). Since the amygdala plays a central role in aversion and freezing behavior, a decreased VTA-amygdala output could code for the aversive nature of the stimulus. As in the striatum, there may be some form of synaptic plasticity in the amygdala that can only be expressed in the absence of DA signaling (Shen et al., 2008).

Most interestingly, the observation that the aversion persisted during the test session suggests a strong learning effect by DA neuron inhibition. Future studies will have to firm up this finding with more elaborate behavioral protocols and test for retention after longer intervals. It will also be important to identify the molecular learning mechanisms engaged by inhibition of DA neurons and parse the contribution of the neurons that are activated by the footshock (Brischoux et al., 2009) and other aversive stimuli (Bromberg-Martin et al., 2010a, 2010b). It will also be important to explore whether addictive drugs that all target the VTA and have been shown to elicit synaptic plasticity in inhibitory transmission will affect the function of GABA neurons in driving the conditioned aversion.

## EXPERIMENTAL PROCEDURES

### Subjects

Experiments were performed on C57BL/6 mice, GIRK2/3$^{-/-}$ mice (Cruz et al., 2008), and GADcre mice. Cre recombinase activity was expressed in all GABAergic interneurons via a cassette encoding Cre inserted into the *Gad2* locus (Kätzel et al., 2011) and THcre mice (Lindeberg et al., 2004). The background strain was C57Bl6 for all mice (>10 generations of backcrossing). The animals were bread in homozygous and heterozygous colonies and used for the experiments between 3 and 8 months of age (22–30 g body weight). Cre$^+$ and cre$^-$ mice from the same litters were used to perform the behavior. All experiments were carried out in accordance with the Institutional Animal Care and Use Committee of the University of Geneva and with permission of the cantonal authorities.

**Figure 3. The Footshock-Induced Inhibition of DA Neurons Is Mediated by $GABA_A$ Receptors**

(A) Single-unit recording, PSTH, and raster plot of a representative putative DA neuron inhibited by an electrical stimulation, recorded in GIRK2/3 KO mice. The inset shows that all recorded cells were inhibited by the stimulus.

(B) Boxplot representation of the response latency, duration and magnitude for wild-type (WT) and GIRK2/3 KO mice, n = 12–24; latency $t_{(28)} = 1{,}21$ $p = 0.24$, duration $t_{(28)} = 1{,}1$ $p = 0.30$, magnitude $t_{(28)} = 0.59$ $p = 0.56$.

(C) Same as in (A) for a representative putative DA cell that was inhibited by the footshock while haloperidol was i.v. injected. The inset shows that all cells were inhibited.

(D) Same as in (B) when saline and haloperidol were i.v. injected to WT mice, n = 5; latency $t_{(29)\ =\ 0.22}$ $p = 0.82$, duration $t_{(29)} = 0.10$ $p = 0.91$, magnitude $t_{(8)} = .0.23$ $p = 0.82$.

(E) Same as in (A) and (C) for a representative putative DA neuron inhibited by an electrical stimulation while saline was applied via a guide cannula implanted above the VTA. The inset shows that all recorded cells were inhibited.

(F) Same representation as in (E) for a representative putative DA neuron not inhibited by an electrical stimulation while bicuculline was applied via a guide cannula implanted above the VTA. The pie chart shows that 90% of putative DA neuron was inhibited and 10% was nonresponsive to the electrical stimulation.

(G) Same as in (B) and (D) for saline and bicuculline in WT mice, n = 6–12; latency $t_{(16)} = 2.02$ ***$p \leq 0.001$, duration $t_{(16)} = 7.68$ ***$p \leq 0.001$, magnitude $t_{(16)} = 4.68$ ***$p \leq 0.001$. Data are expressed as median (line), interquartile (box), and 75$^{th}$ and 25$^{th}$ percentiles and SD (error bars).

See also Figure S3.

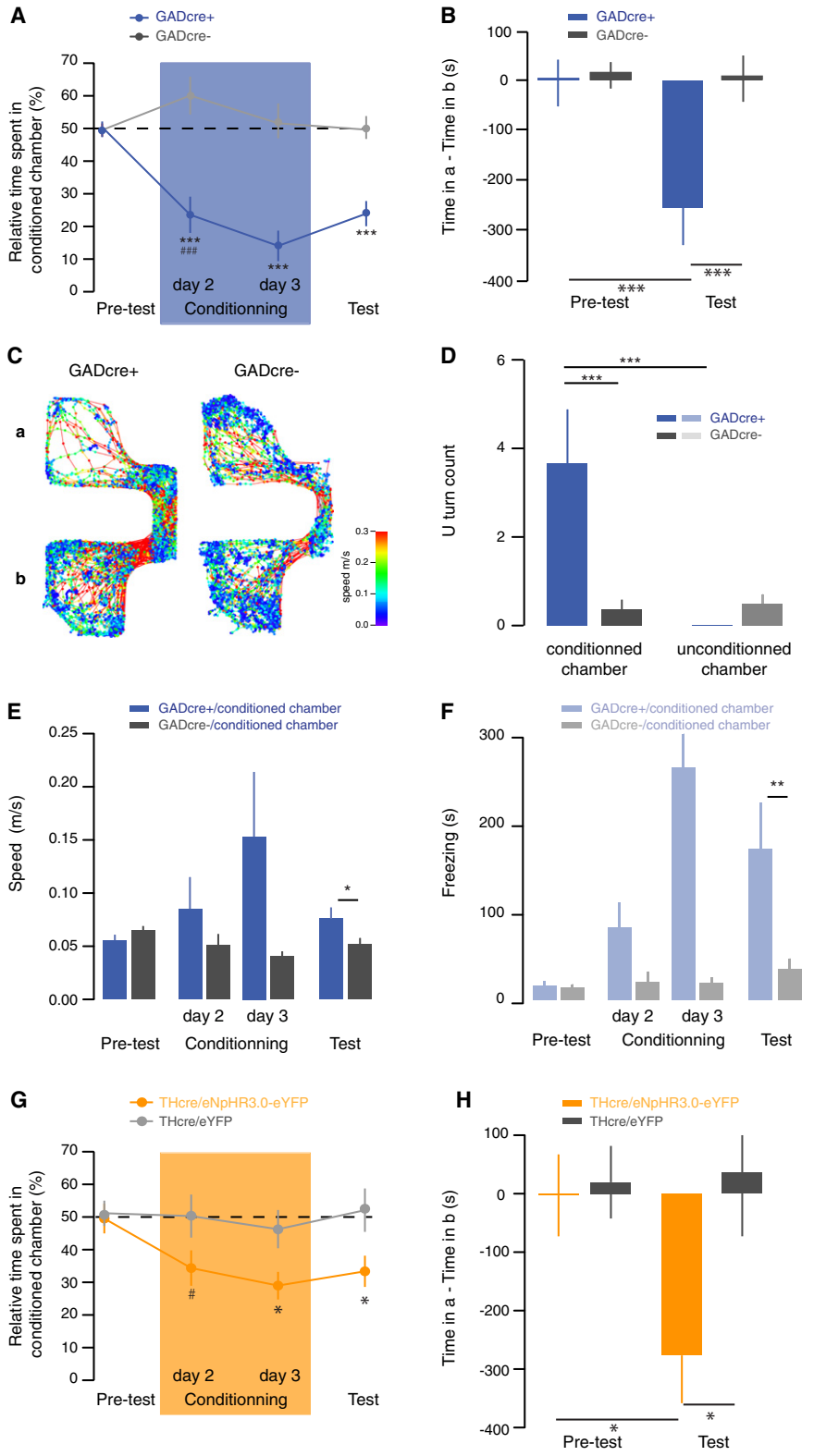


**Figure 4. Indirect or Direct Inhibition of DA Neurons Is Sufficient to Drive Behavioral Aversion**

(A) Aversive learning curve showing the relative time spent in light-paired chamber for each session. The two groups exhibited a significantly different performance ($F_{(1,21)} = 36.02$, $p \leq 0.001$). One conditioning session (blue box) is enough to induce an aversion of the conditioning chamber in GADcre$^+$ mice (###, $t_{(16)} = 4.4$ $p \leq 0.001$). Only GADcre$^+$ mice showed aversion during the whole experiment ($F_{(3,63)} = 9.98$, ***$p \leq 0.001$) (GADcre$^+$ versus GADcre$^-$ on conditioning day 1 $t_{(21)} = 4.4$ ***$p \leq 0.001$; GADcre$^+$ versus GADcre$^-$ on conditioning day 2 ***$p \leq 0.001$, $t_{(5.01;21)}$; GADcre$^+$ versus GADcre$^-$ on test day 1 $t_{(21)} = 4.9$ ***$p \leq 0.001$).

(B) Bar graph showing the aversion difference score measured as time spent in conditioned chamber a – time spent in unconditioned chamber b. Note that during the pretest there is no initial aversion as the time spend by the mice in both chambers is equal. After conditioning, mice expressing ChR2-eYFP in VTA GABA cells show a clear aversion on the test day for the conditioned chamber a (pretest day versus test day for GADcre$^+$ mice $t_{(21)} = 4.9$ ***$p \leq 0.001$ but not control mice (GADcre$^+$ versus GADcre$^-$ on test day $t_{(16)} = 5.74$ ***$p \leq 0.001$ n = 9–14).

(C) Tracking data from a representative trace of a GADcre$^+$ and a GADcre$^-$ mice on the conditioning day 2. The color code corresponds to the speed with blue representing resting state and red fast movement.

(D) Bar graph showing the number of U turn each group of mice made at the entrance of each chamber. This measurement reveals the decision of the GADcre$^+$ mice to avoid the light-paired chamber ($F_{(1,21)} = 14,68$ ***$p \leq 0.001$, GADcre$^+$ versus GADcre$^-$ in conditioned chamber $t_{(21)} = 3.31$ **$p \leq 0.01$, conditioned versus unconditioned chamber for GADcre$^+$ $t_{(18)} = 2.94$ **$p \leq 0.01$).

(E) Bar graph showing the average speed for each group in the conditioned chamber $F_{(1,21)} = 8,47$ ***$p \leq 0.001$, GADcre$^+$ versus GADcre$^-$ on test day $t_{(21)} = 2.1$ *$p \leq 0.05$).

(F) Bar graph showing the time spent in freezing status for each group in the unconditioned chamber ($F_{(1,24)} = 4,38$ ***$p \leq 0.001$, GADcre$^+$ versus GADcre$^-$ on test day $t_{(19)} = 3.18$ **$p \leq 0.01$).

(G) Same as in (A) with THcre$^+$ mice infected in the VTA with AAV5-flox-eNpHR3.0-eYFP or AAV5-flox-eYFP. The two groups exhibited a significantly different performance ($F_{(1,16)} = 5$, $p \leq 0.001$). Two conditioning sessions (amber box) are sufficient to induce an aversion of the conditioning chamber in THcre$^+$/eNpHR3.0-eYFP mice ($t_{(14)} = 3.3$ **$p \leq 0.01$). Only THcre$^+$/eNpHR3.0-eYFP mice showed aversion during the whole experiment ($F_{(3,21)} = 7.7$ ***$p \leq 0.001$) (THcre$^+$/eNpHR3.0-eYFP versus THcre$^+$/eYFP on conditioning day 2 $t_{(16)} = 2.3$ *$p \leq 0.05$; THcre$^+$/eNpHR3.0-eYFP versus THcre$^+$/eYFP on test day $t_{(16)} = 2.2$ *$p \leq 0.05$).

(H) Same as in (B). Note that during the pretest there is no initial aversion as the time spent by the mice in both chambers is equal. After conditioning, mice expressing eNpHR3.0-eYFP in VTA DA cells show a clear aversion on the test day for the conditioned chamber a (pretest day versus test day for THcre$^+$/eNpHR3.0-eYFP mice $t_{(14)} = 2.5$ *$p \leq 0.05$ but not control mice (THcre$^+$/eNpHR3.0-eYFP versus THcre$^+$/eYFP on test day $t_{(16)} = 2.2$ *$p \leq 0.05$ n = 10).

Bars are means ± SD. See also Figure S4.

### Virus Injection

Injections of purified double-floxed AAV5-DIO-ChR2-eYFP, purified double-floxed AAV5-DIO-eNpHR3.0-EYFP, or AAV5-DIO-eYFP virus produced at the University of North Carolina (Vector Core Facility) were made in 3-week-old GADCre or THcre mice. Anesthesia was induced and maintained with isoflurane (Baxter AG, Vienna, Austria) at 5% and 1%, respectively. The mouse was placed in a stereotaxic frame (Angle One; Leica, Germany) and craniotomies were performed bilaterally over the VTA using stereotaxic coordinates (ML ± 0.4 to 0.8, AP −3.4, DV 4.4 from bregma). Injections of viruses were carried out using graduated pipettes (Drummond Scientific Company, Broomall, PA), broken back to a tip diameter of 10–15 μm, at a rate of ∼100 nl $min^{-1}$ for a total volume of 500 nl. In all experiments the virus was allowed a 3 weeks to incubate before any other procedures were carried out.

### Immunohistochemistry

Injected $GADcre^{+}$ mice were anaesthetized with nembutal (50 mg kg) and perfused transcardially with 4% paraformaldehyde in phosphate buffer. The brain was extracted and postfixed for 3 hr, cryoprotected in 30% sucrose in PBS, frozen, and cut at 40 mm with a sliding microtome. From GADcre tissues, dual immunofluorescence with guinea pig antibody against the α1 subunit, a mouse antibody against tyrosine hydroxylase, was performed as previously described (Fritschy and Mohler, 1995) in perfusion-fixed transverse sections from the brain of VTA-ChR2-eYGP-expressing GADcre mice. Images were taken with a laser scanning confocal microscope using a 320 (numerical aperture [NA] 0.8) or a 363 (NA 1.4) objective, using sequential acquisition of separate channels to avoid crosstalk. The same procedure was followed for THcre mice. Localization of DA cell bodies and fibers was confirmed by labeling with chicken anti-tyrosine hydroxylase antibody (1:300). Cell bodies were identified using the 4′,6-diamidino-2-phenylindole, dihydrochloride (DAPI) stain (1:50,000). Transduction efficiency was quantified using a confocal microscope by comparing the EYFP cells with TH immunoreactive cells.

### Electrophysiology in Acute Slices

At least 2 weeks following virus infection, mice were euthanized and horizontal slices from midbrain (250 μm) were prepared in ice cold artificial cerebral spinal fluid (ACSF: [in mM] NaCl 119, KCl 2.5, $MgCl_2$ 1.3, $CaCl_2$ 2.5, $NaH_2PO_4$ 1, $NaHCO_3$ 26.2, and glucose 11 [pH 7.3], continuously bubbled with 95%/5% $O_2/CO_2$). Neurons were visualized with IR camera Gloor Instrument PCO on an Olympus scope (BX51) and whole-cell patch-clamp recordings (Multiclamp 700A amplifier) were made from neurons in the VTA, identified as the region medial to the medial terminal nucleus of the accessory optical tract. The internal solution contained (in mM) K-gluconate 30, KCl 100, $MgCl_2$ 4, creatine phosphate 10, $Na_2$ ATP 3.4, $Na_3$ GTP 0.1, EGTA 1.1, and HEPES 5. Cells were clamped at −60 mV.

### Extracellular Recordings

Mice were anesthetized with chloral hydrate 4% (induction, 480 mg/kg i.p.; maintenance, 120 mg/kg i.p.) and positioned in a stereotaxic frame (MyNeurolab). Body temperature was maintained at 36°C–37°C using a feedback-controlled heating pad (Harvard Apparatus). An incision was made in the midline to expose the skull such that a blur hole was unilaterally drilled above the VTA (coordinates considering a 10° angle: between 3.2 ± 0.3 mm posterior to bregma and 1.3 ± 0.3 mm lateral to midline [Paxinos and Franklin, 2004]), and the dura was carefully retracted. All procedures were performed with the permission of the Cantonal Veterinary Office of Geneva.

Recording electrodes were pulled with a vertical puller (Narishige, Tokyo, Japan) from borosilicate glass capillaries (outer diameter, 1.50 mm; inner diameter, 1.17 mm; Harvard Apparatus). Electrodes were broken back to give a final tip diameter of 1–2 um and filled with one of the following solutions: 0.5% Na-acetate plus 2% Chicago sky blue dye or 0.5 M NaCl plus 20 mM bicuculline methiodide. All electrodes had impedances of 15–25 MΩ. They were angled by 10° from the vertical, slowly lowered through the blurr hole with a micro drive (Luig Neumann) and positioned in the VTA (coordinates: 3.0–3.4 mm posterior from bregma, 1.1–1.4 mm lateral to the midline, 3.9-4.5 mm ventral to pial surface [Paxinos and Franklin, 2004]). Each electrode descend was spaced 100 μm from the others. A reference electrode was placed in the subcutaneous tissue. Electrical signals were AC coupled, amplified, and monitored in real time using a digital oscilloscope and audiomonitor. Signals were digitized at 20 kHz (for waveform analysis) or 5 kHz and stored on hard disk using custom-made program within IGOR (WaveMetrics, Lake Oswego, OR). The band-pass filter was set between 0.3 and 5 kHz.

At the end of each experiment, Chicago sky blue dye was deposited by iontophoresis (−15 uA, 15 min) to mark the final position of the recording site. The mouse was killed with an overdose of chloral hydrate. The brain was removed and frozen in a −20°C solution of methyl butane. Brain coronal sections of 50 μm were cut on a cryostat, stained with luxol fast blue—cresyl violet and the recording site was verified by light microscopy.

### Optical Stimulation

A cleaved end of an optical fiber (200 μm diameter, Thorlabs) was inserted through the guide cannula into the VTA of anesthetized mice. After baseline recording of the spontaneous activity of VTA cells, the laser (light power was controlled to reach no more than 5 mW at the tip of the optical fiber) was switched on for 1 or 2 s continuously and off for 9 or 8 s. This optical stimulation was repeated 50 times.

### Footshock

Footshock was delivered by two 30 gauge needles implanted in the lateral side of the foot controlateral to the neuronal recordings. Electrical stimulations were generated using an isolated pulse stimulator (1–5 mA, 0.1 ms single pulse duration; AM systems) and delivered at a frequency of 0.5 Hz using custom-made program within IGOR (Wavemetrics).

### Drug Administration

Morphine (2 mg/kg), naloxone (1 mg/kg), apomorphine (0.05 mg/k), haloperidol (0.2 mg/kg) were prepared in 0.9% saline and administered intravenously through a 30 gauge cannula inserted in a lateral tail vein. Injection volumes ranged between 30 and 60 μl. Injection of saline had no effect on the firing rate and discharge pattern. Bicuculline methiodide (20 mM) was either applied locally to DA-like neurons via diffusion from the recording electrode as shown previously in vivo (Ji and Shepard, 2007; Tepper et al., 1995) or via a guide cannula (500 nM; Gavello-Baudy et al., 2008). To compare the basal firing rate and discharge pattern with and without drugs, cells were recorded after 10 min of drug diffusion and before delivering the footshocks. These parameters were stable over time indicating that the effect of the drug was rapid in onset and persistent.

### In Vivo Electrophysiology Data Analysis

VTA neurons were recorded for 5 min to establish their basal firing rate and discharge properties before drug administration, footshock delivery, or light stimulation. The processed data were displayed as event raster plots, binned color-coded raster plots, peristimulus time histograms (PSTHs), or firing rate plots. Event raster plots show the time markers of detected activity of 40–50 consecutive footshock or light responses. PSTHs (5 ms bin width) were analyzed to determine excitatory and inhibitory periods as described previously (Jodo et al., 1998). Briefly, baseline values were obtained by calculating the mean and standard deviation (SD) of counts per bin of the 500 ms preceding the footshock or 1 or 2 s preceding the light stimulation. The onset of the response was defined as the first of 5 consecutive bins for which the mean firing rate was more or less that the baseline by 2 SDs. Inhibition was defined as a period of at least 15 bins in which the mean count per bin dropped at least 35% below mean baseline. The magnitude of the excitatory or inhibitory response was normalized to the baseline activity according to the following equation: Magnitude = (counts in response period) − (mean counts per bin in baseline) × (number of bins in response period). The maximal increase in firing rate was determined from the firing rate plot by subtracting the mean baseline from the maximal bin value.

### Conditioned Place Aversion

Behavioral tests were conducted at least 15 days postsurgery. A three-chamber CPP/CPA apparatus was used for the CPA test (Med associates). The two chambers were separated by a corridor and have distinct walls drawings, floor and shape (with an equal surface). A video tracking system

(Anymaze, Stoelting) recorded all animal movements. The paradigm consisted in 3 sessions over 4 days. During all the sessions mice were allowed to freely explore the entire apparatus. CPA protocol consisted of the following sessions: day 1 = 15 min pretest session. Mice were connected to an optical fiber but the lasers were off. Most of the mice (about 85%) did not show side preference before conditioning session. Mice showing unconditioned side preference (staying longer than 200 s more in one chamber) were excluded. Days 2 and 3 = 30 min conditioning sessions were conducted to avoid biased procedure: the light paired chamber was assigned in a counterbalanced order. The laser was continuously activated when mice entered the conditioned chamber for a maximum duration of 30 s to avoid any overheating of the brain structures. If mice keep staying in the conditioned chamber another 1 min, the laser was reactivated for 30 s. Light power was controlled between each animal to be around 5 mW at the tip of the optical fiber (200 μm diameter). Day 4 = all of the mice were allowed to freely explore the chambers as in the conditions of day 1.

### Histology

After completion of the experiment, animals with misplaced cannula or ChR2 expression were excluded from behavioral analysis. The viral injection, although unilateral, also infected GABA neurons in the contralateral VTA, which were probably also activated by the blue light laser.

### Data Analysis and Statistics

Electrophysiological data were analyzed in Igor and Prism, t test was used for statistical analysis. When the data were not normally distributed, a Mann-Whitney test was used. Behavioral data was analyzed using Anymaze, Igor, and Prism. Between and within subjects t tests, and mixed factor repeated-measures ANOVA with planned comparison made by t test were used when applicable with a $p = 0.05$.

## SUPPLEMENTAL INFORMATION

Supplemental Information includes four figures and can be found with this article online at doi:10.1016/j.neuron.2012.02.015.

## ACKNOWLEDGMENTS

We thank Matthew Brown for critical reading of the manuscript. We thank Eoin O'Connor for support in behavioral experiments. We also thank Gero Miesenböck for generously providing the GADcre mice. This study was supported by the National Center of Competences in Research. "SYNAPSY - The Synaptic Bases of Mental Diseases" financed by the Swiss National Science Foundation as well as a core grant to C.L. K.M.T. is supported by NRSA fellowship F32 MH880102 and PILM (MIT). K.D. is supported by the National Institutes of Health, the Howard Hughes Medical Institute, the Defense Advanced Research Projects Agency Reorganization and Plasticity to Accelerate Injury Recovery Program, the Gatsby Charitable Foundation, the Woo, Snyder, and Yu Foundations, and the Wiegers Family Fund. All optogenetic tools and methods are distributed and supported freely (www.optogenetics.org). K.R.T. and C.L. designed the study and wrote the manuscript. K.R.T., C.Y., and G.L. performed the in vivo electrophysiological experiments and analyzed the data. K.R.T. performed the in vitro electrophysiological experiments and analyzed the data. M.T., K.M.T., and J.J.M. performed behavioral experiments in K.D.'s group, and K.D. also provided reagents. J.D. performed immunohistochemistry.

Accepted: February 1, 2012
Published: March 21, 2012

## REFERENCES

Acquas, E., Carboni, E., Leone, P., and Di Chiara, G. (1989). SCH 23390 blocks drug-conditioned place-preference and place-aversion: anhedonia (lack of reward) or apathy (lack of motivation) after dopamine-receptor blockade? Psychopharmacology (Berl.) *99*, 151–155.

Anstrom, K.K., and Woodward, D.J. (2005). Restraint increases dopaminergic burst firing in awake rats. Neuropsychopharmacology *30*, 1832–1840.

Anstrom, K.K., Miczek, K.A., and Budygin, E.A. (2009). Increased phasic dopamine signaling in the mesolimbic pathway during social defeat in rats. Neuroscience *161*, 3–12.

Balcita-Pedicino, J.J., Omelchenko, N., Bell, R., and Sesack, S.R. (2011). The inhibitory influence of the lateral habenula on midbrain dopamine cells: ultrastructural evidence for indirect mediation via the rostromedial mesopontine tegmental nucleus. J. Comp. Neurol. *519*, 1143–1164.

Beckstead, M.J., Grandy, D.K., Wickman, K., and Williams, J.T. (2004). Vesicular dopamine release elicits an inhibitory postsynaptic current in midbrain dopamine neurons. Neuron *42*, 939–946.

Brischoux, F., Chakraborty, S., Brierley, D.I., and Ungless, M.A. (2009). Phasic excitation of dopamine neurons in ventral VTA by noxious stimuli. Proc. Natl. Acad. Sci. USA *106*, 4894–4899.

Bromberg-Martin, E.S., Matsumoto, M., and Hikosaka, O. (2010a). Dopamine in motivational control: rewarding, aversive, and alerting. Neuron *68*, 815–834.

Bromberg-Martin, E.S., Matsumoto, M., and Hikosaka, O. (2010b). Distinct tonic and phasic anticipatory activity in lateral habenula and dopamine neurons. Neuron *67*, 144–155.

Cruz, H.G., Ivanova, T., Lunn, M.-L., Stoffel, M., Slesinger, P.A., and Lüscher, C. (2004). Bi-directional effects of GABA(B) receptor agonists on the mesolimbic dopamine system. Nat. Neurosci. *7*, 153–159.

Cruz, H.G., Berton, F., Sollini, M., Blanchet, C., Pravetoni, M., Wickman, K., and Lüscher, C. (2008). Absence and rescue of morphine withdrawal in GIRK/Kir3 knock-out mice. J. Neurosci. *28*, 4069–4077.

D'Ardenne, K., McClure, S.M., Nystrom, L.E., and Cohen, J.D. (2008). BOLD responses reflecting dopaminergic signals in the human ventral tegmental area. Science *319*, 1264–1267.

Dobi, A., Margolis, E.B., Wang, H.-L., Harvey, B.K., and Morales, M. (2010). Glutamatergic and nonglutamatergic neurons of the ventral tegmental area establish local synaptic contacts with dopaminergic and nondopaminergic neurons. J. Neurosci. *30*, 218–229.

Fadok, J.P., Dickerson, T.M.K., and Palmiter, R.D. (2009). Dopamine is necessary for cue-dependent fear conditioning. J. Neurosci. *29*, 11089–11097.

Fadok, J.P., Darvas, M., Dickerson, T.M.K., and Palmiter, R.D. (2010). Long-term memory for pavlovian fear conditioning requires dopamine in the nucleus accumbens and basolateral amygdala. PLoS ONE *5*, e12751.

Fields, H.L., Hjelmstad, G.O., Margolis, E.B., and Nicola, S.M. (2007). Ventral tegmental area neurons in learned appetitive behavior and positive reinforcement. Annu. Rev. Neurosci. *30*, 289–316.

Flagel, S.B., Clark, J.J., Robinson, T.E., Mayo, L., Czuj, A., Willuhn, I., Akers, C.A., Clinton, S.M., Phillips, P.E.M., and Akil, H. (2011). A selective role for dopamine in stimulus-reward learning. Nature *469*, 53–57.

Fritschy, J.M., and Mohler, H. (1995). GABAA-receptor heterogeneity in the adult rat brain: differential regional and cellular distribution of seven major subunits. J. Comp. Neurol. *359*, 154–194.

Fujisawa, S., and Buzsáki, G. (2011). A 4 Hz oscillation adaptively synchronizes prefrontal, VTA, and hippocampal activities. Neuron *72*, 153–165.

Gavello-Baudy, S., Le Merrer, J., Decorte, L., David, V., and Cazala, P. (2008). Self-administration of the $GABA_A$ agonist muscimol into the medial septum: dependence on dopaminergic mechanisms. Psychopharmacology (Berl.) *201*, 219–228.

Grace, A.A., and Bunney, B.S. (1983). Intracellular and extracellular electrophysiology of nigral dopaminergic neurons—1. Identification and characterization. Neuroscience *10*, 301–315.

Guarraci, F.A., Frohardt, R.J., Young, S.L., and Kapp, B.S. (1999). A functional role for dopamine transmission in the amygdala during conditioned fear. Ann. N Y Acad. Sci. *877*, 732–736.

Hong, S., Jhou, T.C., Smith, M., Saleem, K.S., and Hikosaka, O. (2011). Negative reward signals from the lateral habenula to dopamine neurons are

mediated by rostromedial tegmental nucleus in primates. J. Neurosci. *31*, 11457–11471.

Jhou, T.C., Fields, H.L., Baxter, M.G., Saper, C.B., and Holland, P.C. (2009a). The rostromedial tegmental nucleus (RMTg), a GABAergic afferent to midbrain dopamine neurons, encodes aversive stimuli and inhibits motor responses. Neuron *61*, 786–800.

Jhou, T.C., Geisler, S., Marinelli, M., Degarmo, B.A., and Zahm, D.S. (2009b). The mesopontine rostromedial tegmental nucleus: A structure targeted by the lateral habenula that projects to the ventral tegmental area of Tsai and substantia nigra compacta. J. Comp. Neurol. *513*, 566–596.

Ji, H., and Shepard, P.D. (2007). Lateral habenula stimulation inhibits rat midbrain dopamine neurons through a GABA(A) receptor-mediated mechanism. J. Neurosci. *27*, 6923–6930.

Jodo, E., Chiang, C., and Aston-Jones, G. (1998). Potent excitatory influence of prefrontal cortex activity on noradrenergic locus coeruleus neurons. Neuroscience *83*, 63–79.

Johnson, S.W., and North, R.A. (1992). Opioids excite dopamine neurons by hyperpolarization of local interneurons. J. Neurosci. *12*, 483–488.

Kätzel, D., Zemelman, B.V., Buetfering, C., Wölfel, M., and Miesenböck, G. (2011). The columnar and laminar organization of inhibitory connections to neocortical excitatory cells. Nat. Neurosci. *14*, 100–107.

Kaufling, J., Veinante, P., Pawlowski, S.A., Freund-Mercier, M.-J., and Barrot, M. (2009). Afferents to the GABAergic tail of the ventral tegmental area in the rat. J. Comp. Neurol. *513*, 597–621.

Labouèbe, G., Lomazzi, M., Cruz, H.G., Creton, C., Luján, R., Li, M., Yanagawa, Y., Obata, K., Watanabe, M., Wickman, K., et al. (2007). RGS2 modulates coupling between GABAB receptors and GIRK channels in dopamine neurons of the ventral tegmental area. Nat. Neurosci. *10*, 1559–1568.

Lassen, M.B., Brown, J.E., Stobbs, S.H., Gunderson, S.H., Maes, L., Valenzuela, C.F., Ray, A.P., Henriksen, S.J., and Steffensen, S.C. (2007). Brain stimulation reward is integrated by a network of electrically coupled GABA neurons. Brain Res. *1156*, 46–58.

Lázaro-Muñoz, G., LeDoux, J.E., and Cain, C.K. (2010). Sidman instrumental avoidance initially depends on lateral and basal amygdala and is constrained by central amygdala-mediated Pavlovian processes. Biol. Psychiatry *67*, 1120–1127.

Lindeberg, J., Usoskin, D., Bengtsson, H., Gustafsson, A., Kylberg, A., Söderström, S., and Ebendal, T. (2004). Transgenic expression of Cre recombinase from the tyrosine hydroxylase locus. Genesis *40*, 67–73.

Luo, A.H., Georges, F.E., and Aston-Jones, G.S. (2008). Novel neurons in ventral tegmental area fire selectively during the active phase of the diurnal cycle. Eur. J. Neurosci. *27*, 408–422.

Lüscher, C., and Malenka, R.C. (2011). Drug-evoked synaptic plasticity in addiction: from molecular changes to circuit remodeling. Neuron *69*, 650–663.

Lüscher, C., and Ungless, M.A. (2006). The mechanistic classification of addictive drugs. PLoS Med. *3*, e437.

Paxinos, G., and Franklin, K.B.J. (2004). The Mouse Brain in Stereotaxic Coordinates (San Diego, CA: Academic Press).

Pezze, M.A., and Feldon, J. (2004). Mesolimbic dopaminergic pathways in fear conditioning. Prog. Neurobiol. *74*, 301–320.

Rosenkranz, J.A., Buffalari, D.M., and Grace, A.A. (2006). Opposing influence of basolateral amygdala and footshock stimulation on neurons of the central amygdala. Biol. Psychiatry *59*, 801–811.

Salamone, J.D. (1994). The involvement of nucleus accumbens dopamine in appetitive and aversive motivation. Behav. Brain Res. *61*, 117–133.

Schultz, W. (2010). Dopamine signals for reward value and risk: basic and recent data. Behav. Brain Funct. *6*, 24.

Schultz, W., Dayan, P., and Montague, P.R. (1997). A neural substrate of prediction and reward. Science *275*, 1593–1599.

Shen, W., Flajolet, M., Greengard, P., and Surmeier, D.J. (2008). Dichotomous dopaminergic control of striatal synaptic plasticity. Science *321*, 848–851.

Sun, W. (2011). Dopamine neurons in the ventral tegmental area: drug-induced synaptic plasticity and its role in relapse to drug-seeking behavior. Curr. Drug Abuse Rev. *4*, 270–285.

Tan, K.R., Brown, M., Labouèbe, G., Yvon, C., Creton, C., Fritschy, J.-M., Rudolph, U., and Lüscher, C. (2010). Neural bases for addictive properties of benzodiazepines. Nature *463*, 769–774.

Tepper, J.M., Martin, L.P., and Anderson, D.R. (1995). GABAA receptor-mediated inhibition of rat substantia nigra dopaminergic neurons by pars reticulata projection neurons. J. Neurosci. *15*, 3092–3103.

Ungless, M.A., Magill, P.J., and Bolam, J.P. (2004). Uniform inhibition of dopamine neurons in the ventral tegmental area by aversive stimuli. Science *303*, 2040–2042.

Valenti, O., Lodge, D.J., and Grace, A.A. (2011). Aversive stimuli alter ventral tegmental area dopamine neuron activity via a common action in the ventral hippocampus. J. Neurosci. *31*, 4280–4289.

van Zessen, R., Phillips, J.L., Budygin, E.A., and Stuber, G.D. (2012). Activation of VTA GABA neurons disrupts reward consumption. Neuron *73*, this issue, 1184–1194.

Williams, G.V., and Millar, J. (1990). Concentration-dependent actions of stimulated dopamine release on neuronal activity in rat striatum. Neuroscience *39*, 1–16.

Xia, Y., Driscoll, J.R., Wilbrecht, L., Margolis, E.B., Fields, H.L., and Hjelmstad, G.O. (2011). Nucleus accumbens medium spiny neurons target non-dopaminergic neurons in the ventral tegmental area. J. Neurosci. *31*, 7811–7816.

Yamaguchi, T., Sheen, W., and Morales, M. (2007). Glutamatergic neurons are present in the rat ventral tegmental area. Eur. J. Neurosci. *25*, 106–118.

Zweifel, L.S., Fadok, J.P., Argilli, E., Garelick, M.G., Jones, G.L., Dickerson, T.M.K., Allen, J.M., Mizumori, S.J.Y., Bonci, A., and Palmiter, R.D. (2011). Activation of dopamine neurons is critical for aversive conditioning and prevention of generalized anxiety. Nat. Neurosci. *14*, 620–626.